Published in final edited form as:
J Tissue Eng Regen Med. 2009 January ; 3(1): 1–10. doi:10.1002/term.127.

Evaluation of articular cartilage repair using biodegradable nanofibrous scaffolds in a swine model: a pilot study

Wan-Ju Li[1], **Hongsen Chiang**[2], **Tzong-Fu Kuo**[3], **Hsuan-Shu Lee**[4], **Ching-Chuan Jiang**[2,*], and **Rocky S. Tuan**[1,*]

[1]Cartilage Biology and Orthopaedics Branch, National Institute of Arthritis and Musculoskeletal and Skin Diseases, National Institutes of Health, Department of Health and Human Services, Bethesda, MD 20892, USA

[2]Department of Orthopedic Surgery, National Taiwan University Hospital, Taipei, Taiwan

[3]National Taiwan University Veterinary Hospital, Taipei, Taiwan

[4]Department of Internal Medicine, National Taiwan University, Taipei, Taiwan

Abstract

The aim of this study was to evaluate a cell-seeded nanofibrous scaffold for cartilage repair *in vivo*. We used a biodegradable poly(*ε*-caprolactone) (PCL) nanofibrous scaffold seeded with allogeneic chondrocytes or xenogeneic human mesenchymal stem cells (MSCs), or acellular PCL scaffolds, with no implant as a control to repair iatrogenic, 7 mm full-thickness cartilage defects in a swine model. Six months after implantation, MSC-seeded constructs showed the most complete repair in the defects compared to other groups. Macroscopically, the MSC-seeded constructs regenerated hyaline cartilage-like tissue and restored a smooth cartilage surface, while the chondrocyte-seeded constructs produced mostly fibrocartilage-like tissue with a discontinuous superficial cartilage contour. Incomplete repair containing fibrocartilage or fibrous tissue was found in the acellular constructs and the no-implant control group. Quantitative histological evaluation showed overall higher scores for the chondrocyte- and MSC-seeded constructs than the acellular construct and the no-implant groups. Mechanical testing showed the highest equilibrium compressive stress of 1.5 MPa in the regenerated cartilage produced by the MSC-seeded constructs, compared to 1.2 MPa in the chondrocyte-seeded constructs, 1.0 MPa in the acellular constructs and 0.2 MPa in the no-implant group. No evidence of immune reaction to the allogeneically- and xenogeneically-derived regenerated cartilage was observed, possibly related to the immunosuppressive activities of MSCs, suggesting the feasibility of allogeneic or xenogeneic transplantation of MSCs for cell-based therapy. Taken together, our results showed that biodegradable nanofibrous scaffolds seeded with MSCs effectively repair cartilage defects *in vivo*, and that the current approach is promising for cartilage repair.

Keywords

cartilage tissue engineering; cartilage repair; nanofibre; mesenchymal stem cell; chondrocyte; *in vivo* model

*Correspondence to: Ching-Chuan Jiang, M.D., Ph.D., Orthopedic Surgery, National Taiwan University Hospital, 7 Chung-Shan South Road, Taipei 100, Taiwan. ccj@ccms.ntu.edu.tw or Rocky S. Tuan Cartilage Biology and Orthopaedics Branch, National Institute of Arthritis and Musculoskeletal and Skin Diseases, National Institutes of Health, Building 50, Room 1503, MSC 8022, Bethesda, MD 20892-8022, USA. tuanr@mail.nih.gov.

1. Introduction

Cartilage tissue engineering is an emerging, promising approach to repair articular cartilage defects and to restore joint function in osteoarthritis and other degenerative joint diseases. This approach generally includes an *ex vivo* tissue regeneration process that involves growing chondrocytes or mesenchymal stem cells (MSCs) in a three-dimensional, porous biomaterial scaffold under conditions that promote cartilage formation. In the presence of appropriate biochemical and mechanical stimuli, MCSs and cultured chondrocytes have been shown to generate engineered cartilage that is morphologically and functionally similar to native hyaline cartilage (Kuo *et al.*, 2006). Upon implantation and proper integration of the engineered cartilage with host tissue, functional articular cartilage in the joint may be restored. Tissue engineering is a promising option for the treatment of cartilage defects.

The use of an *in vivo* model is required to assess the feasibility of applying tissue-engineered cartilage for human cartilage repair. A well-designed *in vivo* model can provide useful information on the biological response and properties of the engineered cartilage in the body. Animal experiments are challenging, due to the issues of animal sources, cost, surgical techniques and post-operative care (Reinholz *et al.*, 2004). A variety of animal models have been used to test tissue-engineering products, including rabbit (Shangkai *et al.*, 2007), goat (Quintavalla *et al.*, 2002), pig (Peretti *et al.*, 2006) and dog (Nehrer *et al.*, 1998). Although rabbits are often used because of their wide availability and relatively low cost of maintenance, goats and pigs have a more similar knee joint anatomy to humans, suggesting that these two animals would probably be better animal models. In addition, the thickness of the articular cartilage also needs to be taken into consideration. The average thickness of human articular cartilage is 2.2–2.5 mm, compared to 1.5 mm in pigs and 0.7–1.5 mm in goats, whereas it is 0.3 mm in rabbits (Hembry *et al.*, 2001; Frisbie *et al.*, 2006). Thinner cartilage increases the technical difficulties of implantation of engineered tissue, and the smaller size of the rabbit joint complicates the surgical creation of a critical size defect. For these reasons, we have chosen a swine model in this pilot study to evaluate engineered cartilage *in vivo*.

Biomaterial scaffolds function as artificial extracellular matrix to provide a physical structure to protect cells and guide tissue growth, and interact with cells via cell–matrix interactions (Daley *et al.*, 2008). Chemical composition and physical architecture of a scaffold have been reported to be key parameters that regulate cell activities (Muschler *et al.*, 2004). Using different materials and fabrication methods, many forms of biomaterial scaffolds with distinct properties have been developed for cartilage tissue engineering (Lu *et al.*, 2001). Electrospun nanofibrous scaffolds composed of ultra-fine biodegradable polymeric fibres morphologically similar to natural extracellular matrix have been widely used in tissue engineering and intensively investigated in our laboratory. We have previously reported the fabrication of biodegradable nanofibres as a suitable biomaterial scaffold for cell-based cartilage tissue engineering, and described the *in vitro* physical and biological properties of cartilage engineered using chondrocytes (Li *et al.*, 2006a) and MSCs (Li *et al.*, 2005a). These *in vitro* results suggest that the unique structural properties of nanofibrous scaffolds, such as a high surface area: volume ratio and collagen fibre-mimetic nano-scale fibres, can be translated into biologically favourable properties to enhance cartilage growth (Li *et al.*, 2006a). To evaluate the *in vivo* applicability of cell-seeded nanofibrous scaffolds, we report here the use of a swine model to evaluate cartilage repair *in vivo* by implantation of constructs generated *ex vivo* into iatrogenic defects on femoral condyles.

For clinical applications, autologous cells are generally preferred for tissue engineering, compared to allogeneic or xenogeneic cells, because of concerns over immuno-safety and

disease transmission. However, the advantage of allogeneic and xenogeneic cells is that they are more readily available without additional surgery. Recently, MSCs have been reported to exhibit immunosuppressive properties, specifically suppressing lymphocyte activities (Bartholomew *et al.*, 2002; Di Nicola *et al.*, 2002), prompting the interest of using non-autologous MSCs as cell therapy for disease treatment. Articular cartilage may be considered an ideal tissue for implanting allogeneically or xenogeneically derived tissue-engineered cartilage because the absence of immune cells, as a result of the lack of vasculature and lymphatic vessels in cartilage (Buckwalter *et al.*, 1997). We were thus interested in assessing the feasibility of using allogeneic or xenogeneic cells for cartilage tissue engineering. Another aim of the study is therefore to investigate cell-based cartilage repair using allogeneic chondrocytes and xenogeneic MSCs pre-cultured in nanofibrous scaffolds.

2. Materials and methods

2.1. *In vitro* pre-culture

The protocol for human tissue procurement was approved by the Institutional Review Board of National Taiwan University Hospital and tissue specimens were collected with the informed consent of patients. The animal experimental protocol was approved by the Institutional Animal Experiment Committee of National Taiwan University Hospital. All animal surgeries were performed in a certified operating room at the National Taiwan University Veterinary Hospital under general anaesthesia, using sterile techniques.

Two male and two female 10 month-old Lee-Sung minipigs weighing 21–23 kg were used for the evaluation of repair. For allogeneic chondrocyte isolation, we used another 10 month-old male pig and harvested approximately 35 mg of articular cartilage from the distal radius of the left foreleg stifle joint, following a previously described method (Chiang *et al.*, 2005). The cartilage specimen was processed aseptically, first rinsed with phosphate-buffered saline (PBS), then minced with a scalpel, washed twice with PBS and digested overnight in an enzyme mixture consisting of 0.2% collagenase and 100 μg/ml hyaluronidase. The tissue debris was removed by filtration with a 40 μm sieve. The chondrocytes in the filtrate were pelleted by centrifugation. The chondrocytes were re-suspended and cultured in Dulbecco's modified Eagle's medium (DMEM; Hyclone, Logan, UT, USA) supplemented with 10% fetal bovine serum (FBS; Hyclone) and antibiotics (50 μg/ml streptomycin and 50 IU penicillin/ml; Gibco, Grand Island, NY, USA). Xenogeneic human MSCs were isolated from bone marrow (5–10 ml) of a patient who underwent prosthetic total hip replacement. The detailed harvesting procedure has been described previously (Lee *et al.*, 2003). After isolation, cells were maintained and expanded in culture medium composed of DMEM, 10% FBS and antibiotics (50 μg/ml streptomycin and 50 IU penicillin/ml). Both chondrocytes and MSCs were cultured at 37 °C in a humidified tissue culture incubator containing 5% CO_2. Cells were passaged prior to reaching 80% confluence. Different passage cells were kept separately during culture and were not mixed in later applications. After 3 weeks of culture, chondrocytes at passage 2 and MSCs at passage 1 were ready to seed onto poly(ε-caprolactone) (PCL) nanofibrous scaffolds.

A PCL nanofibrous mat fabricated following the electrospinning method reported previously (Li *et al.*, 2006b) was a three-dimensional, porous structure composed of randomly orientated ultra-fine, nano-scaled fibres (Figure 1A). Uniformly circular nanofibrous scaffolds of 8 mm diameter and 2 mm thickness were cut from the PCL nanofibrous mats, sterilized under UV light for 30 min each side, soaked in 70% ethanol for 30 min and rehydrated with sequential rinses of 50%, 25%, sterile distilled water and finally Hank's balanced salt solution for 30 min each. For cell seeding, trypsin-released cells were reconstituted as a suspension at a density of 4×10^6 cells/ml, and a 0.1 ml aliquot of the cell

suspension was seeded onto a 0.5-cm^2 circular scaffold, i.e. the delivery of 4×10^5 cells, resulting in 8×10^5 cells/cm^2 seeding density on one side of the nanofibrous scaffold. The seeded scaffolds were then placed in 24-well tissue culture plates (Figure 1B) and maintained in a tissue culture incubator. Additional 20 μl aliquots of culture medium were added every 30 min to maintain scaffold wetness. After 2 h, the seeding procedure was repeated to the other side of the scaffold. Each nanofibrous scaffold contained a total of 8×10^5 seeded chondrocytes or MSCs. The cellular constructs were cultured in 10% FBS-supplemented DMEM for additional 21 days before being implanted *in vivo*.

2.2. Implantation of cellular constructs

To reduce the number of animals used in the study and compare the different treatments in the same animal, both knees of the hind legs were operated in the same surgery. Two 7 mm circular, full-thickness cartilage defects were created in the centre of the distal weight-bearing surface of each femoral condyle without damaging the subchondral bone. Thus, a total of 16 defects in eight knees were assigned to four different treatment groups (Table 1). These different treatments were: (a) an allogeneic group, in which allogenenic chondrocyte seeded nanofibrous scaffolds were implanted; (b) a xenogeneic group, in which xenogeneic MSC-seeded nanofibrous scaffolds were implanted; (c) an acellular group, in which nanofibrous scaffolds without chondrocytes or MSCs were implanted; and (d) a no-implant control group, in which the defects received no treatment.

During the operation, no bleeding was observed from the surface of exposed subchondral bone after creating the cartilage defect. Nanofibrous scaffolds were securely attached to the adjacent cartilage with four absorbable sutures around the construct (4-0 Dexon; Sherwood, Davis and Geck, St. Louis, MO, USA). In the immediate postoperative period, the animals were maintained in cages with standard postoperative care. During this period of time, motion of the knee was not restricted and full weight-bearing on the surgical joints was allowed. One week after the surgery, wound healing was verified before the animals were released from the postoperative cage and transferred to individual spaces with good ventilation.

2.3. Macroscopic examination and histological evaluation

Six months after the implantation surgery, the animals were euthanized with overdoses of Pentobarbital for evaluation of the treated femoral condyles. Macroscopically, smoothness and colour at the repair sites were observed and recorded. Each condyle was trisected along the frontal plane to evaluate graft integration to adjacent native cartilage and subchondral bone. The specimens were fixed, decalcified, dehydrated, embedded, sectioned and stained with haematoxylin and eosin (H&E; Sigma, St. Louis, MO, USA).

The regenerated cartilage was scored according to the Visual Histological Assessment Scale published by the International Cartilage Repair Society (ICRS) (Mainil-Varlet *et al.*, 2003). The score is based on the parameters of surface, matrix, cell distribution, cell population viability, subchondral bone and cartilage mineralization (Table 2). All specimens were evaluated in a blinded manner on the basis of one parameter at a time with a score of 0–3 by two independent examiners without discussion. The highest score of 3 was assigned to the ideal repair result and the lowest score of 0 was assigned to the poorest repair result. A representative score for each parameter was determined by averaging the scores of the two examiners and reported separately under each independent parameter.

2.4. Mechanical testing

Mechanical testing was performed on the specimens obtained from the four experimental groups as well as native cartilage. The tensile stress-relaxation property of each specimen

was determined by an unconfined uniaxial indentation test using a custom-designed mechanical tester (Mak *et al.*, 1987; Mow *et al.*, 1989) as described previously (Chiang *et al.*, 2005). After recording the thickness, the specimen was securely mounted on an adjustable stage with precise height control. The stage was raised by a predetermined height, enough to apply a 30% strain on the cartilage surface against a 2 mm diameter bold-tip probe. The response force was recorded as a function of time using a stress gauge on the base of the probe and transformed to compressive stress.

3. Results

To further characterize cell-seeded nanofibre constructs for cartilage tissue engineering and to explore the applicability of the constructs for clinical applications, we used an *in vivo* swine model to evaluate the potential of nanofibre-based engineered cartilage for cartilage defect treatment. In this study, electrospun PCL nanofibrous scaffolds served as a cell carrier to deliver allogeneic chondrocytes or xenogeneic MSCs to iatrogenic cartilage defects and later function as a secure physical structure to stabilize and protect those cells, facilitating cell proliferation and matrix production. The results showed that 6 months after repair the defects treated with different regimens showed various extents of cartilage repair, at both macro- and microscopic levels, as well as differences in mechanical properties.

3.1. Macroscopic observation

Macroscopic observation provided a straightforward assessment of the effectiveness of treatments for cartilage defect repair. The surface smoothness and colour of the regenerated cartilage were compared to those of adjacent native cartilage. Six months after implantation, the defects implanted with chondrocyte-seeded constructs resulted in a large lesion filled with soft yellowish tissue (Figure 2A, left), suggesting that the repair was neither complete nor effective. The acellular constructs did show a small degree of tissue repair (Figure 2A, right; Figure 2B, right; Figure 2C, left), suggesting that acellular nanofibrous scaffolds might have attracted neighbouring cells to facilitate cartilage repair. The human MSC-seeded constructs achieved the most uniform repair, restoring the 7 mm-wide circular defect into a relatively smooth surface (Figure 2B, left). In addition, the colour of the regenerated cartilage tissue was indistinguishable from that of the surrounding host cartilage, suggesting similarity in tissue composition. Defects without implantation remained as shallow holes filled with connective tissue as a result of the spontaneous healing process (Figure 2C, right).

To examine the repair tissue at the defect site beneath the surface of the regenerated cartilage, we trisected the condyle implanted with the MSC-seeded and acellular constructs. The regenerated tissue successfully filled the defect (Figure 3A) and appeared macroscopically homogeneous from the surface to the deeper zone and similar to the surrounding host cartilage. However, the subchondral bone failed to maintain its osseous structure and was replaced by cartilage-like tissue, resulting in the absence of a tidemark between cartilage and bone (Figure 3A). This feature suggested that a significant amount of subchondral bone remodelling occurred during the 6 months post-surgery. Compared to the repair by MSC-seeded constructs, the acellular construct showed similar disruption of subchondral bone, with soft, yellow fibrous connective tissue in the subchondral area (Figure 3B). This was different from the white cartilage-like tissue generated by MSC-seeded constructs.

3.2. Histological analysis

Histological staining showed the extent of cartilage repair at the microscopic level. Cartilage repair by chondrocyte-seeded constructs was incomplete, resulting in a discontinuous

cartilage surface (Figure 4A). After 6 months, there were areas of normal subchondral bone; however, pieces of unabsorbed nanofibres were found interspersed in the subchondroal bone (arrow). In contrast, the MSC-seeded constructs resulted in a smooth and uniform cartilage surface (Figure 4B), consistent with the macroscopic observation (Figure 2B). As observed macroscopically, cartilage was present in the remodelled subchondral region. The cartilage defects implanted with the acellular constructs failed to regenerate substantial cartilage, resulting in an uneven surface (Figure 4C). Also in these specimens, the original subchondral bone was disrupted and filled with fibrous tissue (arrow, Figure 4C). Similar to that found in the chondrocyte-seeded constructs, unabsorbed nanofibres were present in the subchondral bone. The defect-only, no-implant group also showed a large uneven surface at the defect site (Figure 4D). Compared to the defect in Figure 4C,there was more subchondral bone damage and fibrous invagination (Figure 4D), suggesting that the nanofibrous construct might help limit subchondral remodelling.

Cell morphology and matrix structure were analysed to identify the regenerated tissue type. Chondrocytes in the tissue regenerated from the chondrocyte-seeded constructs were round and were positioned within lacunae (Figure 5A). However, the chondrocytes were not as dispersed in large amounts of extracellular matrix as those in native cartilage, suggesting that the regenerated tissue was more fibrocartilaginous in nature. The tissue regenerated from the MSC-seeded constructs contained round, clustered chondrocytes, similar to those found in the surrounding hyaline cartilage (Figure 5B). Mixed fibrochondrocytes and fibrous tissue cells were found in the tissue regenerated from the acellular constructs (Figure 5C). Fibrous tissue cells were found throughout the regenerated tissue except in the region close to host cartilage, in which fibrochondrocytes were found. In the defect-only group, long, spindle-shaped, fibrous tissue cells were found in the regenerated tissue within the defect site, suggesting that only fibrous tissue was formed (Figure 5D).

We used ICRS Visual Histological Assessment to quantitatively compare the regenerative tissue from each group (Figure 6). The system allows the examiners to individually evaluate and report each cartilaginous feature marking ideal cartilage repair, rather than reporting a summed score for an overall cartilage repair. This may be particularly useful to examine and compare regenerated cartilage tissues with varying extents of hyaline cartilaginous features. For surface smoothness, the cartilage surface from the MSC-seeded construct group scored 2.5, the highest of the four groups, suggesting a smoother, integrated cartilage surface. The chondrocyte-seeded construct group, the no-implant group, and the acellular construct group had smoothness values of 1.875, 1.875, and 1.5, respectively. In terms of matrix types, both the chondrocyte- and the MSC-seeded construct groups scored 1.5, indicating more hyaline cartilage than both the acellular construct and the no-implant groups, which scored 1. For cell distribution, more cells were present in the acellular construct group (score = 1.875) and were presented in columnar arrangement than those in the chondrocyte-seeded construct, the MSC-seeded construct and the no-implant groups, scoring 1.5, 1.5 and 1, respectively. For cell viability, all four groups scored 2 or above, suggesting that cells were predominantly viable regardless of treatment. Under the category of subchondral bone, the repair by the acellular constructs scored 2 and showed less subchondral bone remodelling, compared to that in the chondrocyte-seeded constructs (score = 1.875), the no-implant group (score = 1.625), and the MSC-seeded constructs (score = 1.5). Finally, for cartilage mineralization, the regenerated cartilage in the chondrocyte-seeded constructs scored 3, suggesting that there was no pathological mineralization presented. Minor mineralization was found in the MSC-seeded construct group, scoring 2. The other two groups scored 1.5, suggesting more abnormal mineralization. Finally, no sign of immune reaction, such as the presence of macrophages or other immune cells, was observed in any of the groups.

3.3. Mechanical evaluation

Mechanical testing was next used to evaluate the functionality of the regenerated cartilage. Compressive stress relaxation represents time-dependent mechanical response to the applied load. The highest stress peak, representing the viscoelastic stiffness of the specimens, detected was 6.8 MPa from the acellular constructs, followed by 6.5 MPa from both the chondrocyte- and MSC-seeded constructs, and finally by 5.5 MPa from the no-implant group (Figure 7). The stress slowly decayed and finally reached equilibrium in the next 30 min. After reaching equilibrium, cartilage repaired by MSC-seeded constructs showed the highest equilibrium stress of 1.5 MPa, whereas cartilage repaired by the chondrocyte-seeded constructs, the acellular constructs and the no-implant group showed 1.2, 1.0 and 0.2 MPa, respectively.

4. Discussion

Electrospun nanofibres have recently drawn a great deal of attention among tissue engineers and bioengineers for the convenience of using them to produce three-dimensional biomaterial scaffolds (Li *et al.*, 2005b; Christenson *et al.*, 2007). A large number of polymers have been successfully electrospun into nanofibres, and their use to culture tissue-specific cells or multipotential stem cells for various tissue-engineering applications has been reported. These studies suggest that nanofibrous scaffolds function as an artificial ECM, favourably accommodating more cells and supporting biological activities (Li *et al.*, 2006a). Specifically, we previously reported that nanofibrous scaffolds enhanced chondrocytic and chondrogenic activities *in vitro* (Li *et al.*, 2003, 2005a). In this study, we have investigated the potential of nanofibrous scaffolds for cartilage tissue engineering *in vivo*. Our results show that biologically favourable nanofibrous scaffolds acting as a cellular vehicle to deliver cells to cartilage lesions effectively facilitate cartilage repair in a swine model. The 7 mm full-thickness circular defects are partially or fully repaired by the cell-seeded nanofibrous constructs. The MSC-based repair is superior to the chondrocyte-based repair. Although defects with no implantation will spontaneously achieve some healing, the repair is limited and the repair tissue is merely soft fibrous tissue rather than mechanically and biologically sound cartilage. Our findings suggest that biomaterial scaffolds deliver and retain a large quantity of therapeutic cells at the implant site, which enable effective repair of the cartilage defects. Autologous chondrocyte transplantation (ACT) is currently used clinically (Brittberg *et al.*, 1994); however, it has not proved to be as successful as originally predicted (Peterson *et al.*, 2002). One of the major complications causing ineffective repair is cell loss after transplantation (Steinert *et al.*, 2007). Using biomaterial scaffolds, such as nanofibrous scaffolds, the delivered cells are securely retained at the implantation site, thus overcoming the problem of poor cell retention (Tuan 2007; Zheng *et al.*, 2007). The nanofibrous scaffolds also provide physical protection to the cells from friction during joint movement. In comparison, the group without scaffold implantation resulted in the formation of fibrous tissue only, likely reflecting the natural history of incomplete cartilage healing or due to shear forces on the cells unprotected by a biomaterial scaffold.

The MSC-seeded constructs led to the most complete repair of the defects, in which a smooth hyaline-like cartilage surface was reproduced with mechanical properties similar to that of native hyaline cartilage. MSCs are undifferentiated progenitor cells that extensively proliferate in nanofibrous scaffolds during the repair process in response to local growth signals. The MSCs further differentiate into chondrocytes that produce cartilage-specific extracellular matrix to fill the defect. The biological process is thus similar to that believed to take place in surgical procedures, such as microfracture and abrasion arthroplasty, that increase local MSC concentration by creating bleeding bone to allow seepage of marrow-derived cells. Compared to chondrocytes that function mainly for matrix production, undifferentiated MSCs could proliferate more rapidly in the scaffolds, which may result in a

higher cell density for repair. Additionally, the newly differentiated chondrocytes from MSCs may be more active in matrix biosynthesis than the mature chondrocytes from cartilage. Together, the increased cell number and matrix production enhance the MSC-based repair. Our results that MSC-based repairs perform better than chondrocyte-based ones agree with those reported in a previous study (Yan and Yu, 2007). In their rabbit study, Yan *et al.* demonstrate that repaired tissues treated with MSCs appear to have better cell arrangement and integration with surrounding cartilage and less subchondral bone remodelling than did repair tissues generated by chondrocytes. A possible reason of the difference in repair quality suggested by the authors is that MSCs, not mature differentiated chondrocytes, are the target cells stimulated by bioactive molecules released from injured tissues. In this manner, the bioactive molecules drive MSCs to effectively repair the defects.

In the current study, we implanted xenogeneic MSC-based tissue engineered constructs to repair cartilage defects and observed no severe immune rejection from the host animal. Previous studies have also suggested that MSCs are immunosuppressive (Bartholomew *et al.*, 2002; Di Nicola *et al.*, 2002) and that MSC transplantation between individuals or species may provide the foundation of MSC-based therapy for disease treatment. MSCs have immunoregulatory effects suppressing T cell recognition and expansion by inhibiting TNFα and INFγ production (Caplan, 2007). Our results show that upon implantation with human MSCs, porcine cartilage defects are likely repaired by chondrocyte-like cells that have differentiated from human MSCs. Yan and Yu (2007) used human MSCs to repair rabbit cartilage defects, demonstrating that xenogeneic human MSCs are not rejected and are able to carry out complete repair. In another study, Ramallal *et al.* (2004) used pig chondrocytes to repair rabbit cartilage defects. They found that about 30% of pig chondrocytes persisted in the regenerated cartilage, without signs of graft versus host rejections or infiltration by immune cells. This study suggests that xeno-transplantation of chondrocytes could be an alternative treatment for cartilage defects. More studies are required to evaluate the safety of transplantation of allo- and xenogeneic MSCs for tissue regeneration.

Our results show that nanofibre-based scaffolds can be applied to successfully treat surgically created cartilage defects. However, subchondral bone remodelling does occur over the 6 months, as some bone is substituted with cartilage. The tidemark separating cartilage and subchondral bone is lost in the newly regenerated tissue. This phenomenon has also been reported in other studies (Chiang *et al.*, 2005; Pulliainen *et al.*, 2007). Pulliainen *et al.* (2007) noted that chondrocyte-seeded poly-$_{L,D}$-lactic acid scaffolds implanted to treat autologous chondral defects repaired the chondral defects but the subchondral bone was replaced by cartilage. Similar to our finding, another study by Chiang *et al.* (2005) reports that fibrous tissue replaces the subchondral bone in control no-treatment knees, suggesting the destruction of subchondral bone is a biological response to the condition of cartilage absence, and fibrous tissue formation is a natural wound-healing process. Although the mechanism(s) causing subchondral bone remodelling is not known, a possible explanation is that cartilage removal exposes subchondral bone to mechanical loading from joint activities during the healing process. In a living joint, cartilage absorbs compressive loads as high as 20-fold body weight, thus protecting subchondral bone from being damaged. Without the protective cartilage layer, the subchondral bone is at risk of microfracture and bleeding under compressive and shear loads, ultimately leading to subchondral bone remodelling (Nehrer *et al.*, 1998). The natural healing process of the body tends to repair the wound with fibrous tissue, forming a scar-like tissue, as seen in our no implantation group. On the other hand, with cellular implantation, the original seeded cells or those migrating from surrounding tissue develop into fibro- or hyaline cartilage, thus preventing fibrous tissue formation in these groups. Although severe inflammation was not seen in our study, it is known that the degradation of PCL decreases local pH, and may cause a minor

inflammatory reaction (Lowry *et al.*, 1997). Thus, by-products released from the PCL degradation could also have contributed to the destruction of subchondral bone.

Fixation of the engineered cartilage to the defect is critical to treatment success. Suboptimal fixation could cause implant displacement or decreased tissue integration, eventually leading to repair failure. The advantage of using nanofibrous scaffolds over other scaffolds, such as hydrogels, is that fabric-like nanofibrous constructs can be easily fixed to the surrounding cartilage tissue with suture. In this study, four stitches were used at the edge of the constructs to stabilize the engineered cartilage. Moreover, the implantation of nanofibre-based cartilage does not require an extra covering material, such as periosteum used in the current ACT procedure (Brittberg *et al.*, 1994), to secure and protect the implant. Harvesting periosteum does not come without morbidity and complications, and it is thus clinically preferable to avoid the use of periosteum.

5. Conclusions

In this pilot study, we demonstrate that nanofibrous scaffolds effectively deliver therapeutic cells to cartilage lesions and support chondrogenic activity during the cartilage regeneration *in vivo*. The xenogeneic MSC-based treatment favourably repairs cartilage defects and restores biomechanical functions of cartilage, suggesting the potential of MSC xeno- or allo-grafting for cartilage tissue engineering. MSC/nanofibre-based cartilage tissue engineering shows promise for the treatment of cartilage defects.

Acknowledgments

The authors thank Dr Bin-Ru She and Mei-Chiao Lin for providing technical assistance in cell culture work. This work was supported by the Intramural Research Programme of NIAMS, NIH (Z01 AR 41131), the National Taiwan University Hospital (NTUH-92A07), and in part by the Industrial Technology Research Institute (ITRI-IR91-1003).

References

Bartholomew A, Sturgeon C, Siatskas M, et al. Mesenchymal stem cells suppress lymphocyte proliferation in vitro and prolong skin graft survival in vivo. Exp Hematol. 2002; 30:42–48. [PubMed: 11823036]

Brittberg M, Lindahl A, Nilsson A, et al. Treatment of deep cartilage defects in the knee with autologous chondrocyte transplantation. N Engl J Med. 1994; 331:889–895. [PubMed: 8078550]

Buckwalter JA, Mankin HJ. Instructional course lectures, the American Academy of Orthopaedic Surgeons – articular cartilage. Part I: tissue design and chondrocytes-matrix interactions. J Bone Joint Surg Am. 1997; 79:600–611.

Caplan AI. Adult mesenchymal stem cells for tissue engineering versus regenerative medicine. J Cell Physiol. 2007; 213:341–347. [PubMed: 17620285]

Chiang H, Kuo TF, Tsai CC, et al. Repair of porcine articular cartilage defect with autologous chondrocyte transplantation. J Orthop Res. 2005; 23:584–593. [PubMed: 15885479]

Christenson EM, Anseth KS, van den Beucken JJ, et al. Nanobiomaterial applications in orthopedics. J Orthop Res. 2007; 25:11–22. [PubMed: 17048259]

Daley WP, Peters SB, Larsen M. Extracellular matrix dynamics in development and regenerative medicine. J Cell Sci. 2008; 121:255–264. [PubMed: 18216330]

Di Nicola M, Carlo-Stella C, Magni M, et al. Human bone marrow stromal cells suppress T-lymphocyte proliferation induced by cellular or nonspecific mitogenic stimuli. Blood. 2002; 99:3838–3843. [PubMed: 11986244]

Frisbie DD, Cross MW, McIlwraith CW. A comparative study of articular cartilage thickness in the stifle of animal species used in human pre-clinical studies compared to articular cartilage thickness in the human knee. Vet Comp Orthop Traumatol. 2006; 19:142–146. [PubMed: 16971996]

Hembry RM, Dyce J, Driesang I, et al. Immunolocalization of matrix metalloproteinases in partial-thickness defects in pig articular cartilage. A preliminary report. J Bone Joint Surg Am. 2001; 83-A:826–838. [PubMed: 11407790]

Kuo CK, Li WJ, Mauck RL, et al. Cartilage tissue engineering: its potential and uses. Curr Opin Rheumatol. 2006; 18:64–73. [PubMed: 16344621]

Lee HS, Huang GT, Chiang H, et al. Multipotential mesenchymal stem cells from femoral bone marrow near the site of osteonecrosis. Stem Cells. 2003; 21:190–199. [PubMed: 12634415]

Li WJ, Cooper JA Jr. Mauck RL, et al. Fabrication and characterization of six electrospun poly(alpha-hydroxy ester)-based fibrous scaffolds for tissue engineering applications. Acta Biomater. 2006b; 2:377–385. [PubMed: 16765878]

Li WJ, Danielson KG, Alexander PG, et al. Biological response of chondrocytes cultured in three-dimensional nanofibrous poly(epsilon-caprolactone) scaffolds. J Biomed Mater Res A. 2003; 67:1105–1114. [PubMed: 14624495]

Li WJ, Jiang YJ, Tuan RS. Chondrocyte phenotype in engineered fibrous matrix is regulated by fiber size. Tissue Eng. 2006a; 12:1775–1785. [PubMed: 16889508]

Li WJ, Mauck RL, Tuan RS. Electrospun nanofibrous scaffolds: production, characterization, and applications for tissue engineering and drug delivery. J Biomed Nanotech. 2005b; 1:259–275.

Li WJ, Tuli R, Okafor C, et al. A three-dimensional nanofibrous scaffold for cartilage tissue engineering using human mesenchymal stem cells. Biomaterials. 2005a; 26:599–609. [PubMed: 15282138]

Lowry KJ, Hamson KR, Bear L, et al. Polycaprolactone/glass bioabsorbable implant in a rabbit humerus fracture model. J Biomed Mater Res. 1997; 36:536–541. [PubMed: 9294770]

Lu L, Zhu X, Valenzuela RG, et al. Biodegradable polymer scaffolds for cartilage tissue engineering. Clin Orthop Relat Res. 2001; 391(Suppl):S251–S270. [PubMed: 11603709]

Mainil-Varlet P, Aigner T, Brittberg M, et al. Histological assessment of cartilage repair: a report by the Histology Endpoint Committee of the International Cartilage Repair Society (ICRS). J Bone Joint Surg Am. 2003; 85-A(Suppl 2):45–57. [PubMed: 12721345]

Mak AF, Lai WM, Mow VC. Biphasic indentation of articular cartilage-I. Theoretical analysis. J Biomech. 1987; 20:703–714. [PubMed: 3654668]

Mow VC, Gibbs MC, Lai WM, et al. Biphasic indentation of articular cartilage-II. A numerical algorithm and an experimental study. J Biomech. 1989; 22:853–861. [PubMed: 2613721]

Muschler GF, Nakamoto C, Griffith LG. Engineering principles of clinical cell-based tissue engineering. J Bone Joint Surg Am. 2004; 86A:1541–1558. [PubMed: 15252108]

Nehrer S, Breinan HA, Ramappa A, et al. Chondrocyte-seeded collagen matrices implanted in a chondral defect in a canine model. Biomaterials. 1998; 19:2313–2328. [PubMed: 9884045]

Peretti GM, Xu JW, Bonassar LJ, et al. Review of injectable cartilage engineering using fibrin gel in mice and swine models. Tissue Eng. 2006; 12:1151–1168. [PubMed: 16771631]

Peterson L, Brittberg M, Kiviranta I, et al. Autologous chondrocyte transplantation. Biomechanics and long-term durability. Am J Sports Med. 2002; 30:2–12.

Pulliainen O, Vasara AI, Hyttinen MM, et al. Poly-L-D-lactic acid scaffold in the repair of porcine knee cartilage lesions. Tissue Eng. 2007; 13:1347–1355. [PubMed: 17518746]

Quintavalla J, Uziel-Fusi S, Yin J, et al. Fluorescently labeled mesenchymal stem cells (MSCs) maintain multilineage potential and can be detected following implantation into articular cartilage defects. Biomaterials. 2002; 23:109–119. [PubMed: 11762829]

Ramallal M, Maneiro E, Lopez E, et al. Xeno-implantation of pig chondrocytes into rabbit to treat localized articular cartilage defects: an animal model. Wound Repair Regen. 2004; 12:337–345. [PubMed: 15225212]

Reinholz GG, Lu L, Saris DB, et al. Animal models for cartilage reconstruction. Biomaterials. 2004; 25:1511–1521. [PubMed: 14697854]

Shangkai C, Naohide T, Koji Y, et al. Transplantation of allogeneic chondrocytes cultured in fibroin sponge and stirring chamber to promote cartilage regeneration. Tissue Eng. 2007; 13:483–492. [PubMed: 17518599]

Steinert AF, Ghivizzani SC, Rethwilm A, et al. Major biological obstacles for persistent cell-based regeneration of articular cartilage. Arthritis Res Ther. 2007; 9:213. [PubMed: 17561986]

Tuan RS. A second-generation autologous chondrocyte implantation approach to the treatment of focal articular cartilage defects. Arthritis Res Ther. 2007; 9:109. [PubMed: 18021426]

Yan H, Yu C. Repair of full-thickness cartilage defects with cells of different origin in a rabbit model. Arthroscopy. 2007; 23:178–187. [PubMed: 17276226]

Zheng MH, Willers C, Kirilak L, et al. Matrix-induced autologous chondrocyte implantation (MACI): biological and histological assessment. Tissue Eng. 2007; 13:737–746. [PubMed: 17371156]

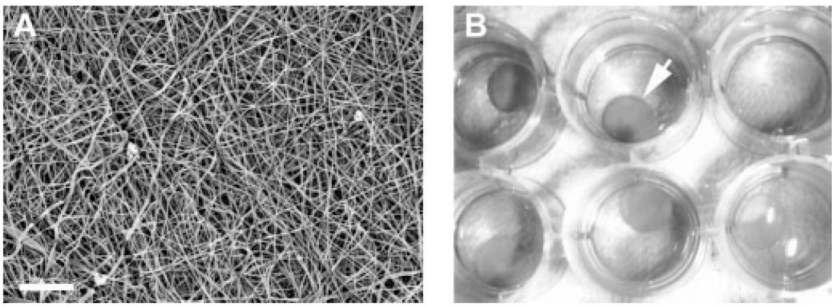

Figure 1.
(A) Structure of electrospun PCL nanofibres examined by scanning electron microscopy. Randomly orientated nano-scaled fibres are seen that define interconnected pores. Bar = 30 μm. (B) Cellular nanofibrous constructs (arrow) with cell culture medium maintained in a 24-well tissue culture plate

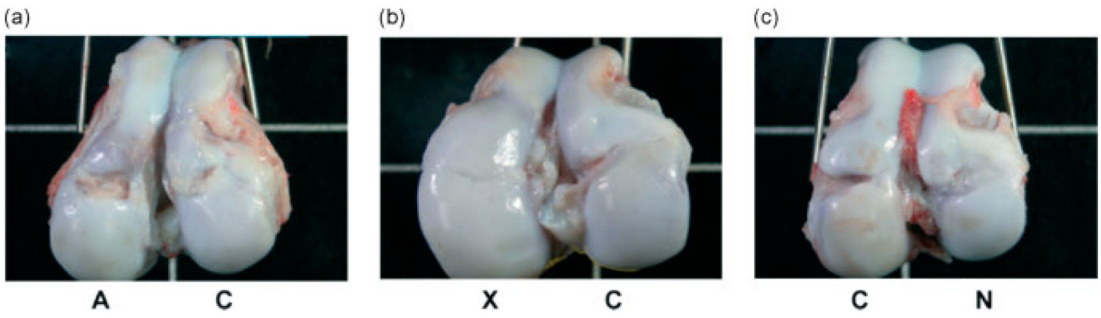

Figure 2.

Gross observation of the repair of swine knees implanted with allogeneic chondrocyte-seeded, xenogeneic human mesenchymal stem cell (MSC)-seeded and acellular constructs, or without implants as the control group at 6 months post-surgery. A, allogeneic chondrocyte-seeded constructs; X, xenogeneic MSC-seeded constructs; C, acellular constructs; N, control no-implant group. MSC-seeded constructs (X) showed successful regeneration of the previously removed cartilage (b). A visible hole partially filled with some fibrous tissue still remained at the surface of the knees repaired by the chondrocyte-seeded constructs (A) and the acellular constructs (C); see panels (a)–(c). The control defect with no implants (N) had a partially repaired lesion filled with tissue (c)

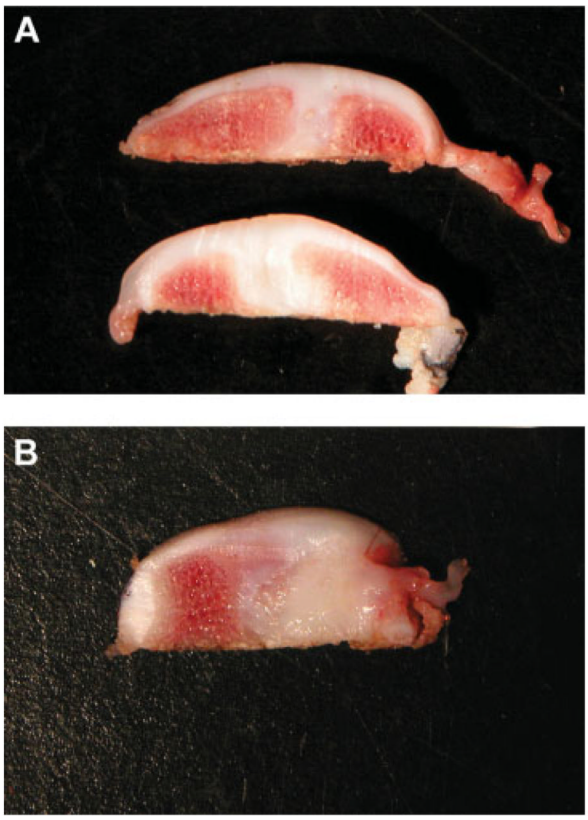

Figure 3.
Cross-sectional view of the trisected knee joint implanted with (A) MSC-seeded or (B) acellular constructs. (A) The defect was fully filled with smooth hyaline cartilage when implanted with the MSC-seeded constructs. The regenerated cartilage filled in the chondral defect as well as appearing in the remodelled subchondral region. (B) The subchondral region of the knee implanted with the acellular construct was filled with yellowish fibrous tissue, consistent with extensive remodelling

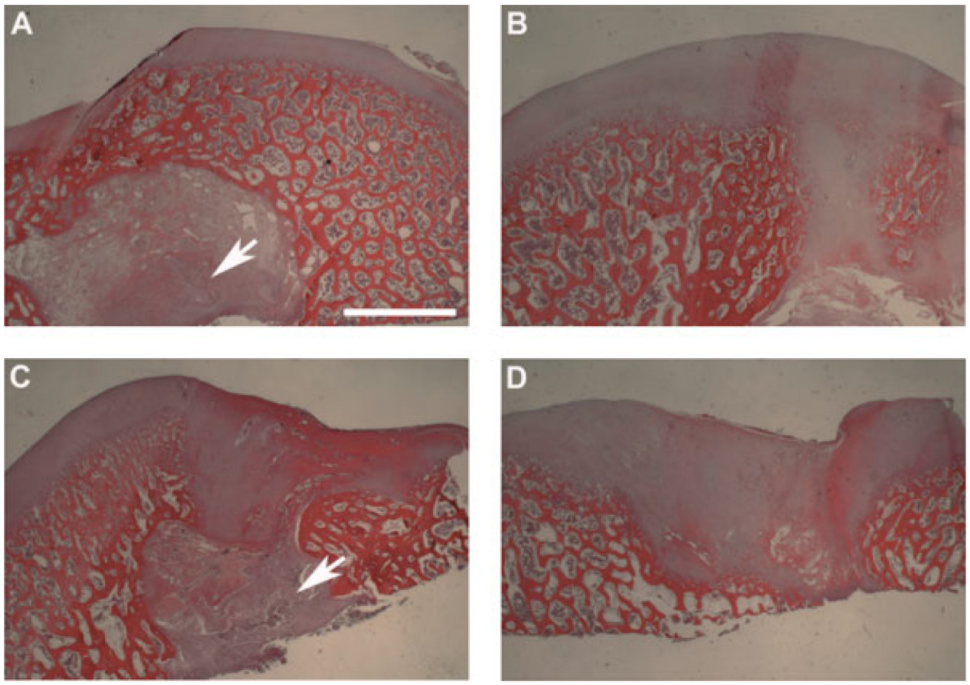

Figure 4.
Histological analysis of cross-sectioned joints implanted with various constructs or no construct. (A) Chondrocyte-seeded construct. A discontinuous cartilage surface was apparent and undegraded polymeric scaffold (arrow) remained in the subchondral bone at the defects. (B) MSC-seeded construct. The regenerated cartilage exhibited a continuous, smooth surface and was slightly thicker compared to the neighbouring native cartilage. (C) Acellular constructs. Irregular cartilage surface and fibrous tissue were evident. Undegraded scaffold (arrow) was found in the subchondral bone. (D) No implantation. A prominent surface groove and fibrous tissue were seen at the defect site. Subchondral bone remodelling was detected in all four groups. Bar = 2 mm

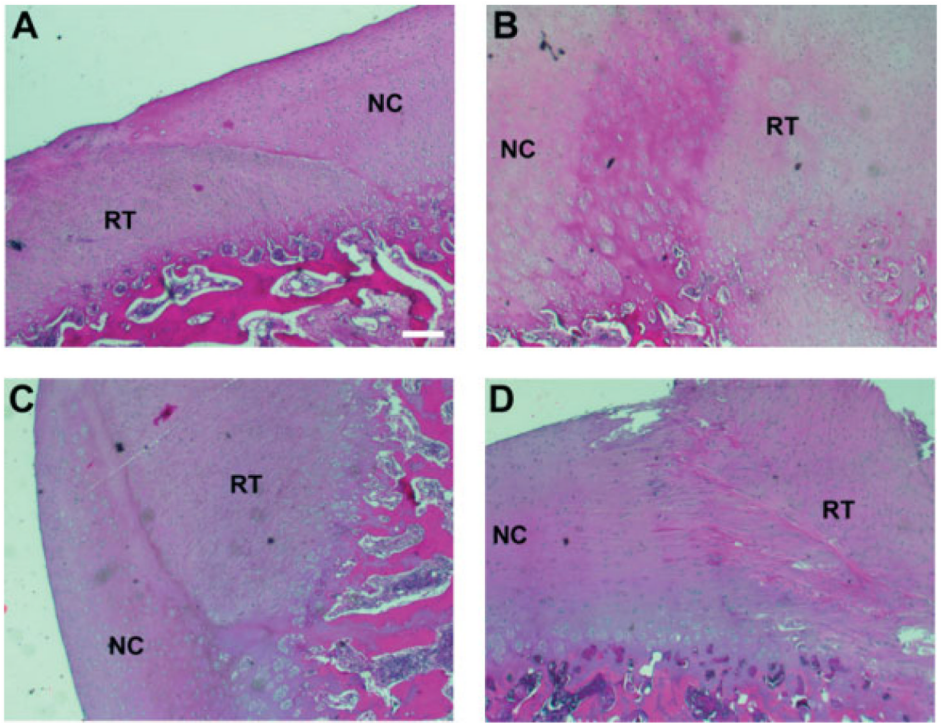

Figure 5.

Histological analysis of cell and matrix morphology in the regenerated tissue formed upon implantation with various constructs or no constructs. (A) Chondrocyte-seeded construct. Cells in the regenerated tissue (RT) appeared to be densely packed fibrocartilage cells surrounded by extracellular matrix that was less dense than that of the surrounding native cartilage (NC). (B) MSC-seeded constructs. Spherical hyaline chondrocytes in the regenerated cartilage formed clusters, similar to those in native cartilage. (C) Acellular constructs. Cells next to the interface were fibrocartilage-like cells and those away from the interface were fibroblasts. (D) No implant. Elongated, fibroblasts in the repair tissue indicate fibrous tissue formation. Bar = 200 μm

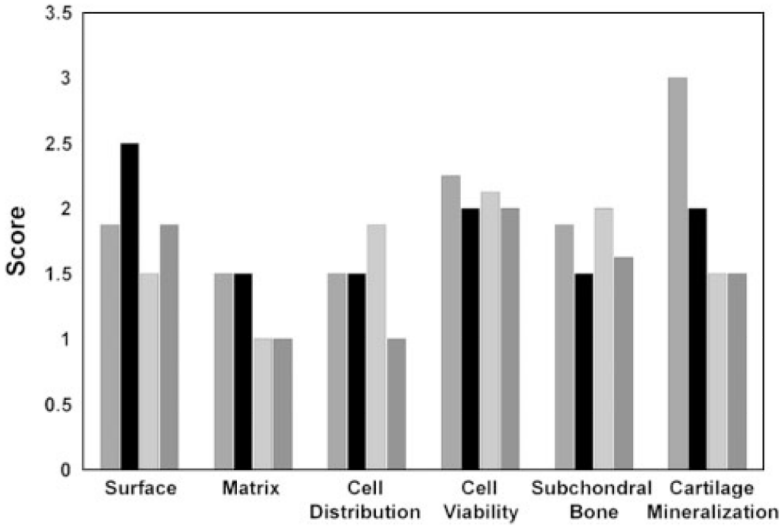

Figure 6.

Quantitative comparison of regenerated tissue between different treatment groups using the ICRS Visual Histological Assessment Scale. The scale ranges from 0 to 3; the higher the score, the closer the regenerated tissue is to normal cartilage. ▒, Chondrocyte-seeded constructs; ■, MSC-seeded constructs; □, acellular constructs; ▒, control no-implant group

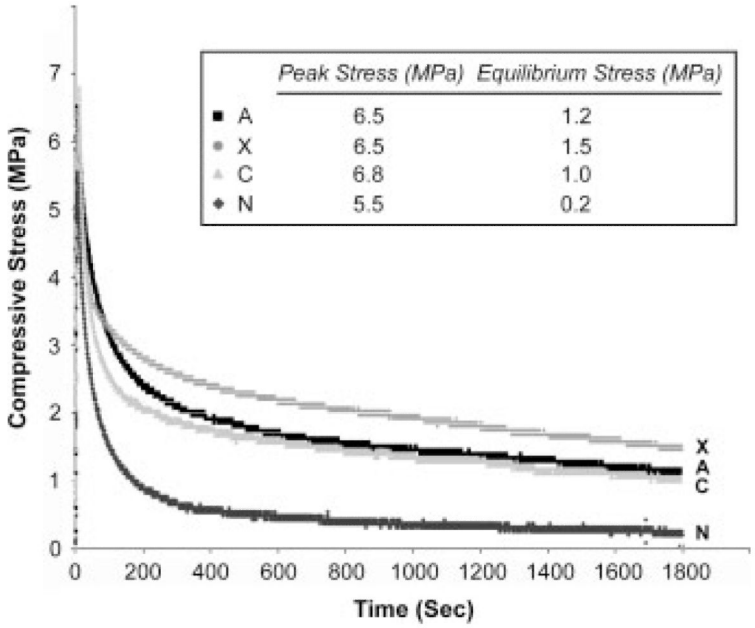

Figure 7.

Compressive stress-relaxation analysis of the mechanical properties of regenerated cartilage from different repair groups. (A) Chondrocyte-seeded constructs; (X) MSC-seeded constructs; (C) acellular constructs; (N) control no-implant group. When reaching equilibrium, cartilage from the MSC-seeded construct group showed the highest compressive stress, followed by cartilage from the chondrocyte-seeded construct group, the acellular construct group, and the control no-implant group

Table 1

Experimental design

No.	Sex	Age (months)	Initial weight (kg)	Treatment			
				Right knee		Left knee	
				Lateral	Medial	Medial	Lateral
1	Male	3	9.6	A	N	A	C
2	Female	3	9.0	C	N	A	A
3	Male	4	8.5	X	C	X	N
4	Female	5	10.1	X	X	C	N

A, allograft; X, xenograft; C, acellular implant; N, no implant.

Table 2
ICRS Visual Histological Assessment Scale*

Feature	Score
Surface	
Smooth/continuous	3
Discontinuous/irregular	0
Matrix	
Hyaline cartilage	3
Hyaline cartilage/fibrocartilage	2
Fibrocartilage	1
Fibrous tissue	0
Cell distribution	
Columnar	3
Columnar/clustery	2
Clustery	1
Individual cells/disorganized	0
Cell viability	
Predominantly viable	3
Partially viable	1
Less than 10% viable	0
Subchondral bone	
Normal	3
Increased remodelling	2
Bone necrosis/granulation tissue	1
Detached/fracture/callus at base	0
Cartilage mineralization	
Normal	3
Abnormal/inappropriate location calcification	0

*Modified from the scale described by Mainil-Varlet *et al.* (2003).